Optimal Location and Sizing of Distributed Generation Units Using NSAGA-III with Heuristic Sampling and Restricted Mating

Huynh Tuyet Vy
Faculty of Electronic Technology, Industrial University of Ho Chi Minh City, Ho Chi Minh City, Vietnam
huynhtuyetvy@iuh.edu.vn

Ho Pham Huy Anh
Ho Chi Minh City University of Technology (HCMUT), 268 Ly Thuong Kiet Street, Dien Hong Ward, Ho Chi Minh City, Vietnam | Vietnam National University Ho Chi Minh City (VNU-HCM), Dong Hoa Ward, Ho Chi Minh City, Vietnam
hphanh@hcmut.edu.vn (corresponding author)

Received: 23 October 2025 | Revised: 15 November 2025 | Accepted: 21 November 2025

 DOI: https://doi.org/10.48084/etasr.15729

ABSTRACT

The integration of Distributed Generation (DG) units in distribution systems is a well-known approach to minimize power losses and improve voltage stability. This research proposes an improved Non-Dominated Sorting Genetic Algorithm (NSGA)-III framework incorporating Heuristic Sampling (HS) for initialization and Restricted Mating (RM) to enhance diversity preservation. The method is benchmarked against the classical NSGA-II, NSGA-III, CMOPSO, and CTAEA methods on the standard IEEE 33-bus and 69-bus test systems. Simulation results demonstrate that the proposed NSGA3-seeded method produces smoother and better-converged Pareto fronts with more uniform solution distribution. Quantitative evaluations using Hypervolume (HV), Generational Distance (GD), and Spacing-to-Extent (StE) indicators confirm consistent improvements in convergence and diversity. Furthermore, the Friedman statistical test confirms that the performance differences among algorithms are statistically significant ($p < 0.05$), and that the proposed NSGA3-seeded consistently attains the best overall ranking across all indicators. The findings confirm the robustness and effectiveness of the proposed approach for practical DG siting and sizing problems.

Keywords-optimal distributed generator allocation; NSGA; CTAEA; heuristic sampling; restricted mating; IEEE distribution systems

I. INTRODUCTION

The growing penetration of Distributed Generation (DG) in active distribution networks has intensified the need for rigorous planning tools that jointly determine siting and sizing decisions to reduce losses, improve voltage profiles, and enhance system reliability [1]. The problem is inherently mixed-integer and multi-objective, with conflicting goals and complex constraints, particularly in unbalanced or meshed systems [2]. A recent study highlights this complexity and the growing adoption of meta-heuristic and Evolutionary Multi-objective Optimization (EMO) methods [3]. For instance, an eco-aware DG planning model using EMOGWO, PSO, RSA, and AOA achieved notable reductions in power loss and emissions [4]. Likewise, DG optimization with GWO, CSA, MOPSO, and GA showed that GWO offered the best efficiency and voltage stability [5]. Within EMO, non-dominated sorting algorithms such as NSGA-II and NSGA-III are widely used for their effectiveness in approximating diverse Pareto fronts [6]. However, studies in power systems still report challenges such as premature convergence and limited diversity near constraint boundaries, reducing Pareto coverage in voltage and stability optimization [7, 8]. These limitations have motivated a wave of recent enhancements, hybrid operators, adaptive selection, and problem-aware search, to improve performance in constrained, high-dimensional spaces [9, 10]. A promising approach integrates domain knowledge into the search process at two levels. Firstly, knowledge-guided initialization (seeding) embeds problem structure from the start, e.g., prioritizing DG buses by load or sensitivity, to enhance early feasibility and speed convergence, as shown across various Multi-Objective Evolutionary Algorithms (MOEAs) and knowledge-assisted searches [2]. Secondly, diversity-aware parent selection (restricted mating) promotes cross-niche recombination to balance exploration and exploitation [11].

Building on these advances, this paper proposes NSGA3-seeded, an improved NSGA-III that integrates two pragmatic enhancements tailored for DG planning: (i) Heuristic Sampling (HS) for load-aware and feasibility-oriented population

initialization [2] and (ii) Restricted Mating (RM), a CTAEA-inspired strategy, for diversity-preserving parent selection during the evolutionary process. Seeding the initial population with problem-aware heuristics has been shown to improve convergence in MOEAs [12]. The RM mechanism is inspired by two-archive constrained MOEAs, where mating is adaptively restricted to maintain feasibility and diversity [13]. Combining a problem-specific seeding strategy and archive-inspired restricted mating has proven effective in recent multi-objective frameworks, improving both early-stage feasibility and long-term diversity [9].

The performance of the proposed algorithm is assessed using three standard indicators—Hypervolume (HV), Generational Distance (GD), and Spacing-to-Extent (StE). These indicators provide a comprehensive assessment of convergence and diversity in MOEAs [14]. To ensure the statistical validity of the results, a non-parametric Friedman test is employed [15, 16]. As demonstrated on the IEEE 33-bus and 69-bus benchmarks, these mechanisms jointly increase the feasible-solution rate and improve both Pareto-front coverage and convergence, compared with baseline NSGA-II/III and contemporary constrained MOEAs. The main contributions of the current paper are:

- Development of a novel NSGA3-seeded algorithm that integrates HS and RM to improve convergence precision, feasibility, and diversity control.
- Comprehensive evaluation on IEEE 33- and 69-bus systems with consistent improvements in the Performance Indicators (PIs) versus NSGA-II/III, CMOPSO and CTAEA.
- Employment of the Friedman test to validate performance differences, demonstrating that the superiority of the NSGA3-seeded is statistically significant across all PIs.

II. PROBLEM FORMULATION

We address the optimal siting and sizing of DG units in radial distribution systems (RDS) under a three-objective framework: (i) minimizing total real power losses, (ii) minimizing system-wide Voltage Deviation (VD), and (iii) maximizing voltage stability via the Voltage Stability Index (VSI). Let N_{bus} be the set of buses and N_{br} be the set of branches in the RDS.

A. Objective 1 - Total Power Losses Minimization

Due to the radial structure, RDS typically incur significant real power losses. Reducing these losses improves energy efficiency and operating economy. The total loss is modeled as the sum of branch losses [17]:

$$f_1 = \min(P_{\text{loss}}) = \min(\sum_{z=1}^{N_{br}} |I_z|^2 R_z) \quad (1)$$

where P_{loss} is the total power losses in the RDS, $|I_z|$ is the absolute value of the current of the z^{th} branch, and R_z represents the resistance of the z^{th} branch.

B. Objective 2 - Total Voltage Deviation Minimization

VD reflects how far bus voltages deviate from a prescribed reference V_{ref}. Excessive deviations can damage equipment and impair normal operation. VD is defined by [18]:

$$f_2 = \min(VD) = \min\left(\sum_{i=1}^{N_{bus}} \left(V_{\text{ref}} - V_i\right)^2\right) \quad (2)$$

C. Objective 3 - Voltage Stability Maximization

Voltage stability is gauged by the voltage stability index (VSI) computed per bus [17]. The system objective is to maximize the lowest VSI:

$$f_3 = \max\left(\min\left(VSI_j\right)\right) = \max\left(\min\begin{pmatrix} V_i^4 - 4\left(P_j R_{ij} + Q_j X_{ij}\right)V_i^2 \\ -4\left(P_j X_{ij} - Q_j X_{ij}\right) \end{pmatrix}\right) \quad (3)$$

where i, j represent the sending and receiving bus, respectively, P_j, Q_j are the active and reactive power of the receiving bus, respectively, and R_{ij}, X_{ij} are the resistance and reactance between buses i, j.

D. Constraints

1) Power Balance

The active-power balance accounts for load demand and network losses:

$$\sum_{i=1}^{N_{DG}} P_{DGi} = P_{\text{loss}} + P_d \quad (4)$$

where N_{DG} is the number of DG units, P_{DGi} is the generated power of the i^{th} DG, P_{loss} represents the total power losses in the RDS, and P_d is the total active load.

2) Operating Limits

DG capacity limits (per unit) are described by:

$$P_{DGi}^{\min} \le P_{DGi} \le P_{DGi}^{\max} \quad (5)$$

Voltage magnitude limits (per bus):

$$V_{\min} \le V_i \le V_{\max}, \forall i \in N_{\text{bus}} \quad (6)$$

III. PROPOSED SOLUTION

We propose NSGA3-seeded, an NSGA-III variant tailored for mixed-integer DG planning in RDS. The algorithm enhances the original NSGA-III with two complementary mechanisms: HS for generating a feasible and load-aware initial population, and RM for feasibility-first and diversity-preserving parent selection. While the core environmental selection, non-dominated sorting combined with reference-direction association, remains identical to the standard NSGA-III, HS and RM operate during initialization and mating stages to improve convergence stability and Pareto-front diversity.

A. Heuristic Sampling

HS is designed to raise the feasible - solution rate and furnish a strong initial population that respects operating limits. Buses are first ranked by active demand (excluding the slack) to form a Top-K shortlist that concentrates siting candidates in load-salient regions. DG locations are then sampled from this shortlist under a non-overlap constraint, ensuring that no two DGs are assigned to the same bus. Let $Load_i$ be the active load demand at the i^{th} bus. For the selected bus set S, DG capacities are allocated proportionally to their local load demands. The allocation ratio for the i^{th} bus is defined as:

$$r_i = \frac{Load_i}{\sum_{j \in S} Load_j}, i \in S \quad (7)$$

The total DG penetration is capped by the operator specification:

$$P_{DG}^{total} = \sum P_{DG} = \alpha P_{sys-load} \quad (8)$$

where $\sum P_{DG}$ is the total DG active power, $P_{sys-load}$ is the system active-load level for the scenario, and $\alpha \in (0,1]$ is an operator-specified cap that limits DG penetration to avoid overvoltage, reverse power flow, and protection-coordination issues.

Each DG unit is then initialized as:

$$P_{DG,i} = r_i \cdot P_{DG}^{total}, i \in S \quad (9)$$

and subsequently clamped to the admissible bounds $P_{\min} \le P_{DG,i} \le P_{\max}$.

A final repair step enforces the uniqueness of locations, bounds the total capacity within the penetration limit, and applies fast voltage checks. If any violation is detected, resampling or adjustment is performed to restore feasibility.

B. Restricted Mating

In conventional NSGA-III, the mating process is typically performed without constraints, i.e., parent solutions are randomly selected from the mating pool based on their ranks and crowding distance. Although this free mating scheme ensures high genetic diversity, it may also lead to the generation of offspring with weak feasibility or limited improvement potential when solving complex multi-objective problems such as DG allocation in distribution networks. In particular, the lack of restrictions can cause mismatches between parent solutions that are highly dissimilar in terms of location, capacity, or objective performance, resulting in inefficient search behavior and slower convergence.

To address this limitation, we integrate an RM mechanism into the NSGA-III. The proposed strategy imposes additional constraints on parent selection, where a candidate pair is only permitted if certain compatibility conditions are satisfied. Specifically, parent solutions are compared based on (i) the spatial distance between DG placement sites, to avoid unrealistic offspring with scattered allocations, (ii) DG capacity similarity, to ensure that offspring inherit balanced operational characteristics, and (iii) multi-objective fitness correlation, so that promising solutions with comparable trade-offs are more likely to recombine. By incorporating these conditions into the mating process, the search is guided toward generating offspring with higher feasibility and competitive quality, while still maintaining sufficient population diversity. This restricted mating strategy enhances the exploitation capability of NSGA-III and improves the convergence speed and stability of the optimization process.

1) Spacial Distance

The parent solutions are desired to be neither too dissimilar (as scattered siting patterns may yield infeasible or poor hybrids) nor too similar (which would prevent effective exploration). Let the decision vector (candidate solution) be:

$$x = \left\{ s_1, s_2, ..., s_{N_{DG}^{\max}}, c_1, c_2, ..., c_{N_{DG}^{\max}} \right\}$$

where s_i and c_i represent the location and capacity of the i^{th} DG unit, respectively, and $N_{DG}^{\max}$ be the maximum number of the integrated DG units.

The spatial difference between two parent solutions x_A and x_B is measured as follows:

$$D_{site}(x_A, x_B) = 1 - \frac{|S(x_A) \cap S(x_B)|}{|S(x_A) \cup S(x_B)|} \in (0,1) \quad (10)$$

where $S(x_A)$ and $S(x_B)$ are the location vectors of candidates x_A and x_B, respectively.

A candidate pair is accepted for mating if and only if the site-difference ratio lies within the prescribed interval:

$$D_{site}^{\min} \le D_{site}(x_A, x_B) \le D_{site}^{\max} \quad (11)$$

2) DG Capacity Similarity

In addition to siting compatibility, parent solutions must also exhibit comparable DG capacity profiles. A large discrepancy in total installed DG capacity between two parents often leads to offspring that violate network operating constraints (e.g., feeder overload or voltage limit violations). Let the total installed DG capacity of solution x be defined as:

$$P(x) = \sum_{i=1}^{N_{DG}^{\max}} p_i \quad (1)$$

where p_i is the rated DG power integrated into the i^{th} bus.

For two parent solutions x_A and x_B, the relative total capacity difference is measured as:

$$\Delta p(x_A, x_B) = \frac{|P(x_A) - P(x_B)|}{\max\{P(x_A), P(x_B)\}} \quad (13)$$

The pair is accepted for mating only if:

$$\Delta p\left(x_A, x_B\right) \le \varepsilon \tag{14}$$

where $\varepsilon \in (0,1)$ is a predefined threshold. This constraint ensures that parent solutions have sufficiently similar DG capacities, thereby reducing the likelihood of producing infeasible offspring and improving the stability of the evolutionary search.

3) Fitness-Based Compatibility Restriction

To guide the mating process toward producing offspring with both quality and diversity, we impose a distance-based restriction in the objective space. Let $f\left(x\right)$ denote the objective vector of parent solution x. If two parents have objective vectors that are too close in the Pareto space, their recombination is unlikely to introduce new diversity and is therefore rejected. Conversely, if the two parents are too far apart (e.g., one is of extremely high quality while the other is very poor), recombination often produces inferior or infeasible offspring, and is also rejected.

The restriction is formalized as a distance condition:

$$d_{fit}^{\min} \le \left\| f\left(x_A\right) - f\left(x_B\right) \right\| \le d_{fit}^{\max} \tag{15}$$

where $\|\bullet\|$ is the Euclidean norm, $d_{fit}^{\min}$ is the minimum allowable distance to avoid redundant mating, and $d_{fit}^{\max}$ is the maximum allowable distance to prevent destructive recombination.

Since the objective values of DG allocation differ in scale and units, all objectives are first normalized into the interval [0,1] using the current estimates of the ideal and nadir points. The Euclidean distance between two parents in the normalized objective space is then used as the basis for the fitness-based restriction. To avoid redundant mating between nearly identical parents, the minimum distance threshold $d_{fit}^{\min}$ is set as a fraction of the average pairwise distance within the population, typically in the range of 10–30%. Conversely, to prevent destructive recombination between parents that are excessively distant in objective space, the maximum threshold $d_{fit}^{\max}$ is set relative to the distribution of distances, commonly chosen between 70–90% of the maximum observed value. In practice, both thresholds are updated adaptively at each generation based on the current population statistics, ensuring that the RM mechanism remains effective throughout the evolutionary search. This adaptive calibration balances diversity preservation and convergence, guiding NSGA-III to explore the Pareto front more efficiently.

C. The Proposed NSGA3-Seeded

Figure 1 illustrates the workflow of the proposed algorithm. The procedure begins with the initialization of the system and algorithm parameters, including network data, population size, and objective functions. During initialization, HS is adopted to create a diverse and feasible initial population, ensuring good coverage of the search space while maintaining system constraints such as voltage limits and DG penetration levels.

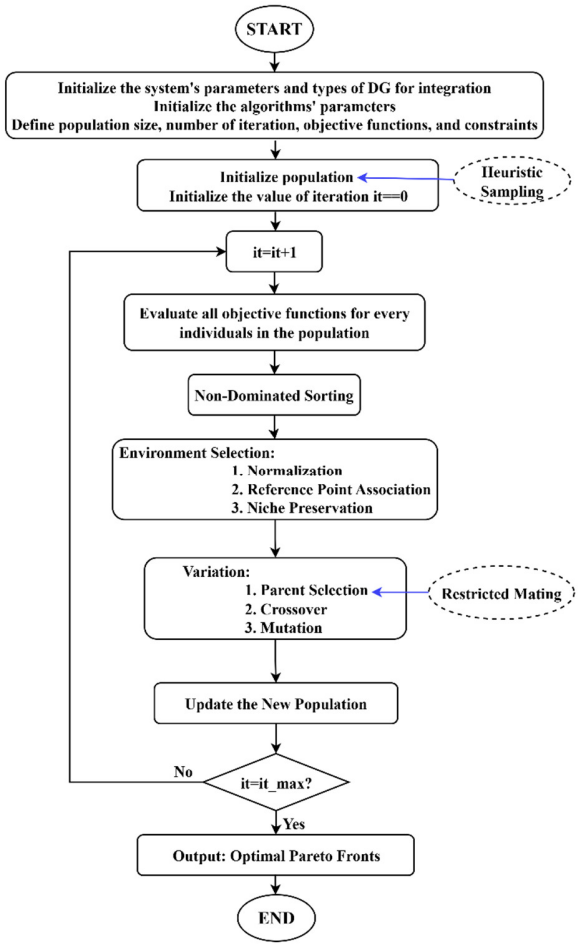

Fig. 1. Workflow of the proposed NSGA3-seeded.

Each individual in the population is evaluated based on a set of multi-objective evaluation functions. The algorithm then performs non-dominated sorting and environment selection, consisting of normalization, reference point association, and niche preservation, to identify elite solutions and maintain population diversity. In the variation phase, an RM mechanism is incorporated into the parent selection process to enhance convergence behavior. The RM strategy operates in three adaptive stages according to the evolution progress:

- Stage 1 (0–20% of total generations): Parent selection is constrained only by spatial distance, promoting exploration by preventing unrealistic scattered placements.
- Stage 2 (20–50%): Both spatial distance and DG capacity similarity are enforced, ensuring that offspring inherit compatible operational characteristics.
- Stage 3 (50–100%): Parent pairing further incorporates fitness correlation to guide the search toward locally optimal regions near the Pareto front.

To ensure adequate exploration and constraint satisfaction, the algorithm monitors the feasibility ratio (Fg), defined as the proportion of feasible individuals in the current population that satisfy all system constraints. If $Fg < 0.4$ after stage 2, it

dynamically increases the capacity thresholds (ε) by 10%, or resets the spatial distance range to $d_{site}^{\min}=0$, $d_{site}^{\max}=1$, thereby preventing premature convergence and maintaining a viable search space. After crossover and mutation, the new population is updated and iteratively refined until the maximum number of generations is reached. Finally, the algorithm outputs the optimal Pareto fronts, representing the best trade-offs among all objectives.

IV. SIMULATION RESULTS AND DISCUSSION

The simulation is performed with three integrated DGs. Comparative analyses were conducted on both IEEE 33-bus and 69-bus test systems. The proposed NSGA3-seeded algorithm was benchmarked against four well-known MOEAs, including NSGA-II, standard NSGA-III, CMOPSO and CTAEA, using identical parameter settings. The obtained Pareto front is evaluated in terms of quality, diversity, and convergence using standard multi-objective PIs, such as HV, GD, and StE [19, 20]. To further assess the reliability of the obtained performance improvements, a non-parametric statistical analysis was conducted using the Friedman test, which is widely adopted for evaluating multiple algorithms across repeated experiments. This test determines whether the observed performance differences among algorithms are statistically significant. The analysis was performed on all three PIs, HV, GD, and STE, for both IEEE 33-bus and 69-bus systems, based on ten independent runs of each algorithm, using a 95% confidence level ($\alpha = 0.05$).

A. Simulation Data

The backward-forward method of power flow analysis was used to determine the voltage and current at the buses in the distribution system. All compared algorithms (NSGA-II, NSGA-III, CMOPSO, and CTAEA) were implemented and executed under identical simulation settings within the same Python environment using the Pymoo framework [19]. The simulation parameters are listed in Table I. All algorithms were run with a fixed maximum iteration limit of 500 and a convergence tolerance threshold based on fitness variation ($<10^{-5}$ over 20 consecutive generations). Each algorithm was independently executed 10 times with different random seeds to account for stochastic variability, and the PIs were obtained from the Pareto fronts of these runs for statistical comparison. Unlike the proposed NSGA3-seeded, which applies HS for problem-aware initialization, all the other algorithms used purely random population initialization.

The IEEE 33 - bus system consists of 33 buses (or nodes), numbered from 1 to 33, and a total of 32 lines connecting the buses. The IEEE 69-bus system consists of 69 buses, numbered from 1 to 69, and 68 lines. Except for the source bus, each bus has a specific load (real power and reactive power), representing electrical appliances and households. Each line has parameters such as reactance and resistance, simulating the physical properties of the conductors. The IEEE 33-bus and 69-bus systems, which are presented in Figures 2 and 3, have a radial configuration. They are designed with a typical rated voltage of 12.66 kV and their parameters are referred in [21, 22].

TABLE I. SIMULATION PARAMETERS

General Parameters	
Max iterations	500
Population size	100
Number of DGs	03
Capacity limits of DGs	0.1 MW-10 MW
Specified value V_{ref}	1 p.u
Operator-specified cap α	0.5
Capacity threshold ε	0.001
Individual Parameters for each MH algorithm	
NSGA-II NSGA-III	n_offsprings = 10 (number of offsprings to generate through recombination). Simulated Binary Crossover (SBX) crossover operator: prob=0.9 (the probability of executing the crossover), eta=15 (the distance parameters of the crossover distribution). Polynomial Mutation (PM) operator: prob=0.9 (probability of mutation for each gene of an offspring), eta = 20 (distance parameter to control the shape of the mutation distribution. Larger values generate offspring closer to the parents).
CTAEA	Used the Das-Dennis method to get reference directions in an M-dimensional space (M=3, 3 objectives): n_points = 91 (number of points on the unit simplex); SBX operator: prob=1.0, eta=30; PM operator: prob=0.9, eta = 20.
CMOPSO	max_velocity_rate: 0.2; max_elite_size: 10; initial_velocity: random; mutate_rate: 0.5.

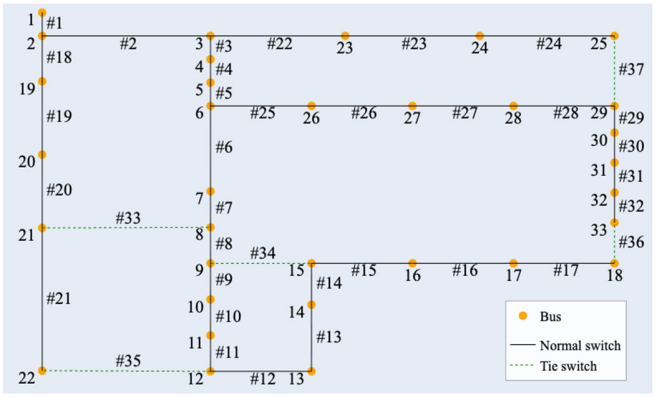

Fig. 2. The IEEE 33-bus system.

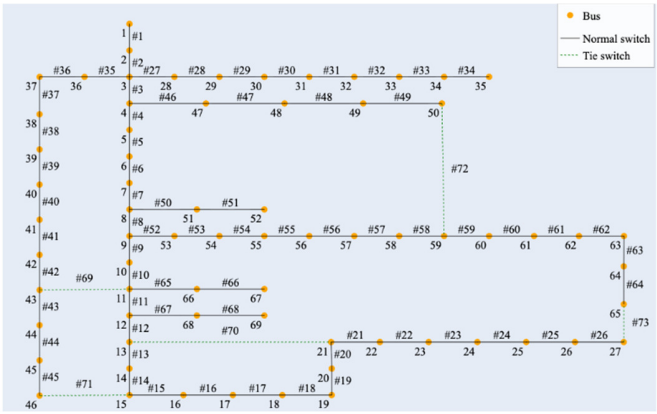

Fig. 3. The IEEE 69-bus system.

B. Simulation Results

1) Pareto Front Analysis

As illustrated in Figures 4 and 5, the Pareto fronts obtained for the IEEE 33-bus and 69-bus systems provide clear visual evidence of the differences in convergence and diversity among the five algorithms. The convergence toward the true Pareto boundary can be assessed by observing how closely the nondominated solutions approach the region characterized by low power loss and VD values along with a high VSI. In both test systems, the solutions obtained by CTAEA and NSGA3-seeded form a smooth, well-defined curved front located near this optimal region, indicating stronger convergence behavior. In contrast, the solutions of NSGA-II and NSGA-III appear scattered and less aligned with the boundary, suggesting premature convergence or insufficient exploitation of the search space.

The uniformity of solution distribution along the Pareto front reflects the algorithm's ability to maintain population diversity. In this aspect, CTAEA and NSGA3-seeded exhibit a more even and continuous spread of points across the front, avoiding large gaps or clusters. CMOPSO achieves wide coverage but shows irregular density, while NSGA-II and NSGA-III present noticeable sparsity in several regions of the objective space. The heuristic sampling and restricted mating strategies embedded in NSGA3-seeded clearly contribute to preserving population diversity, ensuring a more balanced exploration of the trade-offs among the objectives.

2) Performance Indicators Comparison

HV, GD, and StE were considered for performance comparison among the applied algorithms. A higher HV value signifies better convergence and a well-distributed Pareto front, reflecting the algorithm's ability to cover a larger portion of the objective space. A lower GD value indicates improved convergence, as the solutions are closer to the reference Pareto front, demonstrating higher proximity to optimality. Similarly, a low StE value suggests a well-distributed Pareto front, with solutions that are uniformly spaced across the objective space.

It should be noted that the HV and GD indicators require the availability of a true Pareto optimal front or a reference front. Since the true front is not known for the considered problem, a reference front is constructed in such a way that each algorithm is executed for 10 independent runs, resulting in a total of obtained Pareto fronts from the applied algorithms. All non-dominated solutions from these fronts are merged into a single solution set. The reference front is then generated by identifying and retaining only the non-dominated solutions within this combined set, ensuring a representative approximation of the true Pareto front for subsequent performance comparison.

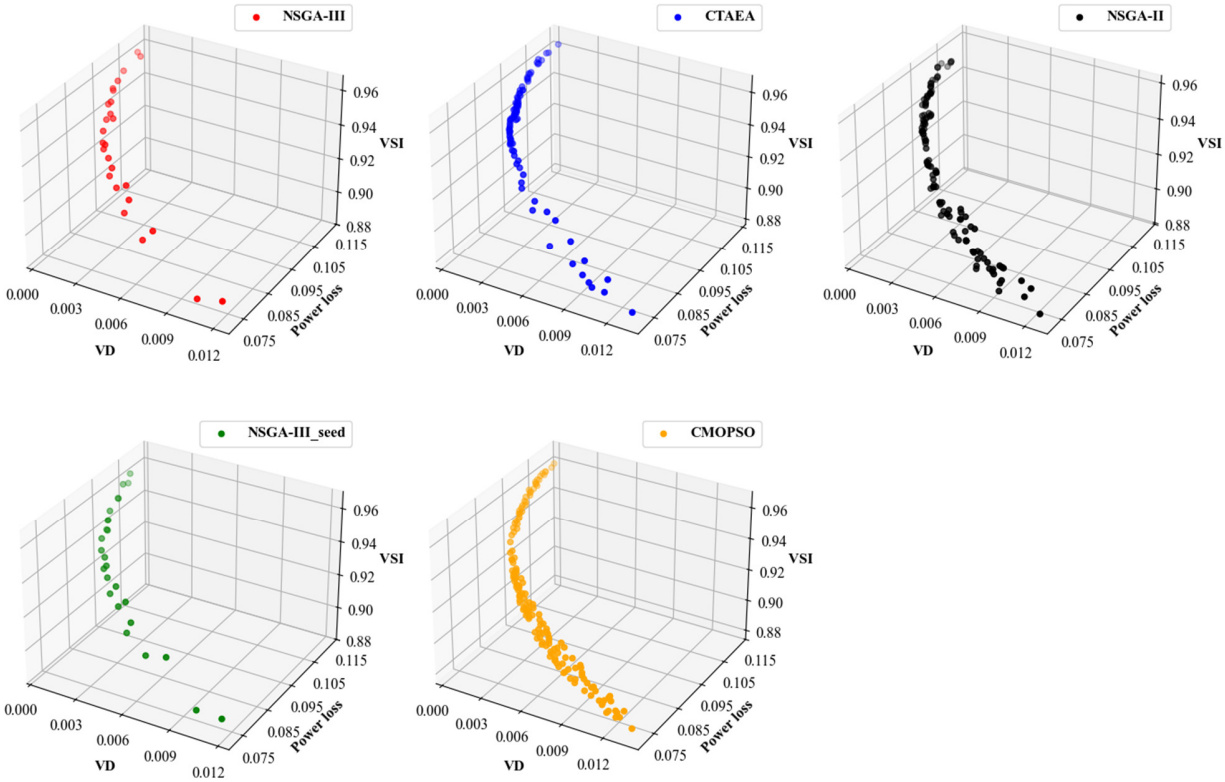

Fig. 4. Pareto fronts obtained from the 33-bus network.

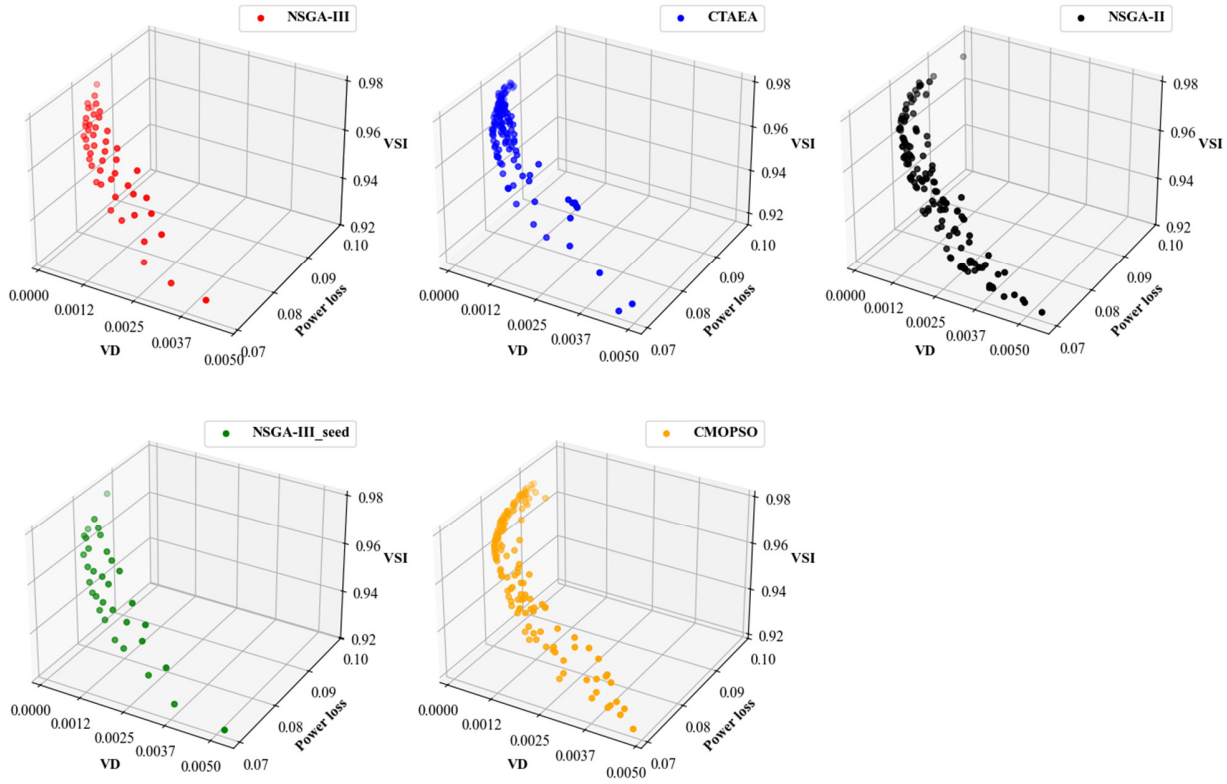

Fig. 5. Pareto fronts obtained from the 69-bus network.

Table II presents the PIs of the proposed NSGA3-seeded algorithm compared to several well-known multi-objective optimization techniques, CMOPSO, NSGA-II, NSGA-III, and CTAEA, on the IEEE 33-bus and 69-bus distribution networks.

In both test systems, the proposed NSGA3-seeded algorithm consistently outperformed the other algorithms. It achieved the highest HV values (0.00335 and 0.00227 for the 33-bus and 69-bus systems, respectively), indicating a superior convergence-diversity balance and broader coverage of the Pareto front. The GD values are also the lowest among all algorithms (0.00032 and 0.00017), suggesting that the obtained Pareto solutions are closest to the true Pareto front. Additionally, the StE metric, which reflects solution distribution uniformity, shows that NSGA3-seeded maintains a more consistent spread of solutions (0.36735 and 0.46504), outperforming the other methods in both networks.

3) Statistical Validation Using the Friedman Test

To further verify the reliability of the obtained performance improvements, a non-parametric Friedman test was applied to statistically evaluate the differences among all five algorithms. The Friedman test is widely adopted in evolutionary optimization studies to assess statistical significance across multiple algorithms and PIs without assuming normality of data distributions [15, 16]. The test was performed on the HV, GD, and StE indicators for both systems, based on 10 independent runs of each algorithm, using a 95% confidence level ($\alpha = 0.05$). The results of the Friedman test are summarized in Table III. All p-values are below 0.05, indicating that the performance differences among the algorithms are statistically significant. This confirms that the improvements achieved by the NSGA3-seeded are not random but statistically meaningful, reflecting genuine algorithmic advantages.

Following the Friedman test, average ranks were calculated to evaluate the relative performance of each algorithm across all indicators. As presented in Table IV, the proposed NSGA3-seeded obtained the lowest (best) average rank of 1.07, outperforming the other methods. CTAEA and NSGA-III ranked second and third, while CMOPSO and NSGA-II showed the weakest performance.

TABLE II. PIs OF THE PROPOSED NSGA3-SEEDED IN IEEE 33-BUS AND 69-BUS NETWORKS

No.	Algorithm	IEEE 33 -bus			IEEE 69 -bus		
		HV	GD	StE	HV	GD	StE
1	CMOPSO	0.00319	0.00373	0.47883	0.00214	0.00079	0.57041
2	NSGA-II	0.00315	0.00268	0.70526	0.00209	0.00047	0.61649
3	NSGA-III	0.00321	0.00053	0.50462	0.00211	0.00026	0.52038
4	CTAEA	0.00324	0.00043	0.59359	0.00219	0.00019	0.70316
5	NSGA3-seeded	0.00335	0.00032	0.36735	0.00227	0.00017	0.46504

TABLE III. STATISTICAL VALIDATION OF PERFORMANCE INDICATORS USING THE FRIEDMAN TEST ($\alpha = 0.05$)

System	IEEE 33 -bus			IEEE 69 -bus		
Indicator	**HV**	**GD**	**StE**	**GD**	**HV**	**StE**
p-value	0.0021	0.0047	0.0035	0.0030	0.0062	0.0029

TABLE IV. AVERAGE PERFORMANCE INDICATOR ALGORITHM RANKS BASED ON THE FRIEDMAN TEST

Algorithm	IEEE 33 -bus			IEEE 69 -bus			Average rank
	HV rank	GD rank	StE rank	HV rank	GD rank	StE rank	
CMOPSO	4.0	4.0	3.5	4.0	4.0	3.8	3.88
NSGA-II	4.8	4.5	5.0	5.0	5.0	4.7	4.83
NSGA-III	3.0	3.0	2.5	3.0	3.0	2.8	2.88
CTAEA	2.2	2.0	2.3	2.0	2.0	2.5	2.17
NSGA3-seeded	1.0	1.0	1.2	1.0	1.0	1.2	1.07

C. Discussion

Overall, the proposed NSGA3-seeded approach demonstrates remarkable convergence precision and diversity maintenance. By integrating HS and RM, the enhanced NSGA-III effectively balances exploration and exploitation throughout the optimization process. HS improves the quality of the initial population, while RM enhances offspring feasibility and accelerates convergence toward a well-distributed Pareto front. The Friedman analysis clearly demonstrates that the proposed algorithm consistently ranks first in all PIs, highlighting its superior convergence speed, solution feasibility, and diversity maintenance. Together with the statistical validation results ($p < 0.05$), these findings provide strong evidence that the proposed modifications to NSGA-III significantly improve optimization quality and robustness for DG planning applications.

V. CONCLUSIONS

This study presented the NSGA3-seeded, an enhanced NSGA-III framework for optimal siting and sizing of DG units in radial distribution systems. The main novelty lies in combining Heuristic Sampling (HS) for problem-aware initialization and Restricted Mating (RM) for diversity-preserving parent selection. The HS mechanism accelerates convergence by embedding load-aware and voltage-feasible heuristics at initialization, while the RM mechanism adaptively balances exploration and exploitation across evolutionary stages. Comprehensive tests on the IEEE 33-bus and 69-bus benchmark systems show that NSGA3-seeded outperforms NSGA-II, NSGA-III, CMOPSO, and CTAEA across all performance indicators (HV, GD, and StE). The algorithm achieves higher HV, lower GD, lower StE, and more uniform Pareto-front distribution. Moreover, the Friedman test further confirms the statistical significance ($p < 0.05$) of these improvements, establishing the reliability of the observed performance gains. These results confirm that integrating domain knowledge and adaptive mating enhances optimization robustness for practical DG planning.

ACKNOWLEDGMENT

We acknowledge Ho Chi Minh City University of Technology (HCMUT), VNU-HCM for supporting this study.

REFERENCES

[1] S. M. Tercan, A. Demirci, Y. E. Unutmaz, O. Elma, and R. Yumurtaci, "A comprehensive review of recent advances in optimal allocation methods for distributed renewable generation," *IET Renewable Power Generation*, vol. 17, no. 12, pp. 3133–3150, 2023, https://doi.org/10.1049/rpg2.12815.

[2] M. Kumar *et al.*, "Optimal Multi-Objective Placement and Sizing of Distributed Generation in Distribution System: A Comprehensive Review," *Energies*, vol. 15, no. 21, Oct. 2022, https://doi.org/10.3390/en15217850.

[3] A. M. Nassef *et al.*, "Review of Metaheuristic Optimization Algorithms for Power Systems Problems," *Sustainability*, vol. 15, no. 12, Jun. 2023, Art. no. 9434, https://doi.org/10.3390/su15129434.

[4] K. C. Phuoc, L. H. Pham, T. N. Ton, T. A. Le, and T. N. T. Huyen, "Multi-Objective Optimization of Emissions and Green Accounting Costs in Smart Distribution Networks with Distributed Generation," *Engineering, Technology & Applied Science Research*, vol. 15, no. 5, pp. 27781–27787, Oct. 2025, https://doi.org/10.48084/etasr.13578.

[5] T. N. Ton, H. H. Lai, L. V. Pham, and T. N. Hoang, "Optimization of Distributed Generation Planning to Maximize the Absorption Rate of Renewable Energy in Distribution Networks," *Engineering, Technology & Applied Science Research*, vol. 15, no. 3, pp. 23008–23013, Jun. 2025, https://doi.org/10.48084/etasr.10921.

[6] H. Ma, Y. Zhang, S. Sun, T. Liu, and Y. Shan, "A comprehensive survey on NSGA-II for multi-objective optimization and applications," *Artificial Intelligence Review*, vol. 56, no. 12, pp. 15217–15270, Dec. 2023, https://doi.org/10.1007/s10462-023-10526-z.

[7] W. Long *et al.*, "A constrained multi-objective optimization algorithm using an efficient global diversity strategy," *Complex & Intelligent Systems*, vol. 9, no. 2, pp. 1455–1478, Apr. 2023, https://doi.org/10.1007/s40747-022-00851-1.

[8] S. Dutta, R. Mallipeddi, and K. N. Das, "Hybrid selection based multi/many-objective evolutionary algorithm," *Scientific Reports*, vol. 12, no. 1, Apr. 2022, Art. no. 6861, https://doi.org/10.1038/s41598-022-10997-0.

[9] Y. Tian, Z. Shi, Y. Zhang, L. Zhang, H. Zhang, and X. Zhang, "Solving optimal power flow problems via a constrained many-objective co-evolutionary algorithm," *Frontiers in Energy Research*, vol. 11, Oct. 2023, https://doi.org/10.3389/fenrg.2023.1293193.

[10] C. A. Nallolla *et al.*, "Multi-Objective Optimization Algorithms for a Hybrid AC/DC Microgrid Using RES: A Comprehensive Review," *Electronics*, vol. 12, no. 4, Feb. 2023, Art. no. 1062, https://doi.org/10.3390/electronics12041062.

[11] K. Li, R. Chen, G. Fu, and X. Yao, "Two-Archive Evolutionary Algorithm for Constrained Multiobjective Optimization," *IEEE Transactions on Evolutionary Computation*, vol. 23, no. 2, pp. 303–315, Apr. 2019, https://doi.org/10.1109/TEVC.2018.2855411.

[12] J. O. Agushaka, A. E. Ezugwu, J. O. Agushaka, and A. E. Ezugwu, "Initialisation Approaches for Population-Based Metaheuristic Algorithms: A Comprehensive Review," *Applied Sciences*, vol. 12, no. 2, Jan. 2022, Art. no. 896, https://doi.org/10.3390/app12020896.

[13] J. Liang, Z. Chen, Y. Wang, X. Ban, K. Qiao, and K. Yu, "A dual-population constrained multi-objective evolutionary algorithm with variable auxiliary population size," *Complex & Intelligent Systems*, vol. 9, no. 5, pp. 5907–5922, Oct. 2023, https://doi.org/10.1007/s40747-023-01042-2.

[14] R. Tanabe and K. Li, "Quality Indicators for Preference-Based Evolutionary Multiobjective Optimization Using a Reference Point: A Review and Analysis," *IEEE Transactions on Evolutionary Computation*, vol. 28, no. 6, pp. 1575–1589, Sep. 2024, https://doi.org/10.1109/TEVC.2023.3319009.

[15] J. Liu and Y. Xu, "T-Friedman Test: A New Statistical Test for Multiple Comparison with an Adjustable Conservativeness Measure," *International Journal of Computational Intelligence Systems*, vol. 15, no. 1, Apr. 2022, Art. no. 29, https://doi.org/10.1007/s44196-022-00083-8.

[16] Z. Ma, G. Wu, P. N. Suganthan, A. Song, and Q. Luo, "Performance assessment and exhaustive listing of 500+ nature-inspired metaheuristic algorithms," *Swarm and Evolutionary Computation*, vol. 77, Mar. 2023, Art. no. 101248, https://doi.org/10.1016/j.swevo.2023.101248.

[17] S. A. Adegoke, Y. Sun, A. S. Adegoke, and D. Ojeniyi, "Optimal placement of distributed generation to minimize power loss and improve voltage stability," *Heliyon*, vol. 10, no. 21, Nov. 2024, Art. no. e39298, https://doi.org/10.1016/j.heliyon.2024.e39298.

[18] N. Saxena, M. Pandit, and L. Srivastava, "Multi-objective DG placement in radial distribution systems using the IbI logic algorithm," *Frontiers in Energy Research*, vol. 12, Nov. 2024, https://doi.org/10.3389/fenrg.2024.1453715.

[19] N. Saxena, M. Pandit, and L. Srivastava, "Multi-objective DG placement in radial distribution systems using the IbI logic algorithm," *Frontiers in Energy Research*, vol. 12, pp. 89497–89509, Nov. 2024, https://doi.org/10.3389/fenrg.2024.1453715.

[20] K. Shang, H. Ishibuchi, L. He, and L. M. Pang, "A Survey on the Hypervolume Indicator in Evolutionary Multiobjective Optimization," *IEEE Transactions on Evolutionary Computation*, vol. 25, no. 1, pp. 1–20, Oct. 2021, https://doi.org/10.1109/TEVC.2020.3013290.

[21] S. H. Dolatabadi, M. Ghorbanian, P. Siano, and N. D. Hatziargyriou, "An Enhanced IEEE 33 Bus Benchmark Test System for Distribution System Studies," *IEEE Transactions on Power Systems*, vol. 36, no. 3, pp. 2565–2572, Feb. 2021, https://doi.org/10.1109/TPWRS.2020.3038030.

[22] H. R. E. H. Bouchekara, Y. Latreche, K. Naidu, H. Mokhlis, W. M. Dahalan, and M. S. Javaid, "Comprehensive Review of Radial Distribution Test Systems for Power System Distribution Education and Research," *Resource-Efficient Technologies*, no. 3, pp. 1–12, Dec. 2019, https://doi.org/10.18799/24056529/2019/3/196.